



Heriot-Watt University
Research Gateway

The quadratic Zeeman effect used for state-radius determination in neutral donors and donor bound excitons in Si:P

Citation for published version:

Litvinenko, KL, Li, J, Stavrias, N, Meaney, AJ, Christianen, PCM, Engelkamp, H, Homewood, KP, Pidgeon, CR & Murdin, BN 2016, 'The quadratic Zeeman effect used for state-radius determination in neutral donors and donor bound excitons in Si:P', *Semiconductor Science and Technology*, vol. 31, no. 4, 045007.
<https://doi.org/10.1088/0268-1242/31/4/045007>

Digital Object Identifier (DOI):

[10.1088/0268-1242/31/4/045007](https://doi.org/10.1088/0268-1242/31/4/045007)

Link:

[Link to publication record in Heriot-Watt Research Portal](#)

Document Version:

Publisher's PDF, also known as Version of record

Published In:

Semiconductor Science and Technology

General rights

Copyright for the publications made accessible via Heriot-Watt Research Portal is retained by the author(s) and / or other copyright owners and it is a condition of accessing these publications that users recognise and abide by the legal requirements associated with these rights.

Take down policy

Heriot-Watt University has made every reasonable effort to ensure that the content in Heriot-Watt Research Portal complies with UK legislation. If you believe that the public display of this file breaches copyright please contact open.access@hw.ac.uk providing details, and we will remove access to the work immediately and investigate your claim.

The quadratic Zeeman effect used for state-radius determination in neutral donors and donor bound excitons in Si:P

This content has been downloaded from IOPscience. Please scroll down to see the full text.

2016 Semicond. Sci. Technol. 31 045007

(<http://iopscience.iop.org/0268-1242/31/4/045007>)

View [the table of contents for this issue](#), or go to the [journal homepage](#) for more

Download details:

IP Address: 86.16.113.208

This content was downloaded on 02/03/2016 at 19:15

Please note that [terms and conditions apply](#).

The quadratic Zeeman effect used for state-radius determination in neutral donors and donor bound excitons in Si:P

K L Litvinenko¹, Juerong Li¹, N Stavrias², A J Meaney³, P C M Christianen³, H Engelkamp³, K P Homewood¹, C R Pidgeon⁴ and B N Murdin¹

¹Advanced Technology Institute and SEPNet, Department of Physics, University of Surrey, Guildford GU2 7XH, UK

²Radboud University, Institute for Molecules and Materials, FELIX Laboratory, Toernooiveld 7c, NL-6525 ED Nijmegen, The Netherlands

³High Field Magnet Laboratory (HFML—EMFL), Radboud University, Toernooiveld 7, 6525 ED Nijmegen, The Netherlands

⁴Institute of Photonics and Quantum Sciences, SUPA, Heriot-Watt University, Edinburgh EH14 4AS, UK

E-mail: k.litvinenko@surrey.ac.uk

Received 22 October 2015, revised 20 January 2016

Accepted for publication 29 January 2016

Published 2 March 2016



CrossMark

Abstract

We have measured the near-infrared photoluminescence spectrum of phosphorus doped silicon (Si:P) and extracted the donor-bound exciton (D^0X) energy at magnetic fields up to 28 T. At high field the Zeeman effect is strongly nonlinear because of the diamagnetic shift, also known as the quadratic Zeeman effect (QZE). The magnitude of the QZE is determined by the spatial extent of the wave-function. High field data allows us to extract values for the radius of the neutral donor (D^0) ground state, and the light and heavy hole D^0X states, all with more than an order of magnitude better precision than previous work. Good agreement was found between the experimental state radius and an effective mass model for D^0 . The D^0X results are much more surprising, and the radius of the $m_j = \pm 3/2$ heavy hole is found to be larger than that of the $m_j = \pm 1/2$ light hole.

Keywords: magneto-optics, impurity in silicon, quadratic Zeeman effect, donor bound exciton

1. Introduction

Study of the quadratic Zeeman effect (QZE) in atoms is of interest in two widely different areas. In astrophysics, estimating the immense magnetic fields generated by highly compact objects requires spectroscopy and fitting to the QZE of hydrogen. In a group IV silicon crystal, atoms are tetrahedrally bonded so that a group V donor such as phosphorus has one unused electron, which orbits around the ion core in the same way as in the hydrogen atom. In such semiconductor impurities the QZE is important at fields easily accessible in laboratory conditions and so understanding is important for interpretation of many magneto-optical and magneto-transport

experiments. The difficulty in calculating the energy levels of hydrogen atoms and hydrogenic impurities in a magnetic field is that the Coulomb field and the magnetic field have different symmetry, so Schrodinger's equation is non-separable, thus some type of approximation is required. There is a characteristic field, when the Coulomb (binding) energy and the magnetic (cyclotron) energy are equal, B_0 , that determines the strength of the QZE. For free hydrogen atoms B_0 is very large, so in most applications the magnetic field is low enough that the QZE can be neglected (i.e. $B \ll B_0$), and the linear Zeeman splitting is an adequate description. In semiconductors the dielectric constant and electron effective mass greatly reduce the characteristic magnetic field B_0 , e.g. for silicon $B_0 = 32.8$ T [1], whereas it is even smaller for most III–V semiconductors. Here we investigate the QZE for Si:P.

One of the best known theoretical approaches to describe experimentally observed spectra of impurities atoms in



Original content from this work may be used under the terms of the [Creative Commons Attribution 3.0 licence](https://creativecommons.org/licenses/by/3.0/). Any further distribution of this work must maintain attribution to the author(s) and the title of the work, journal citation and DOI.

semiconductors is the effective mass theory (EMT), see for example [2, 3]. EMT assumes slowly varying wavefunctions and it is very successful for the large excited states. The accuracy can be improved by including more bands and/or taking into account the existence of multiple equivalent conduction-band valleys (six in silicon). However it is less accurate for prediction of the ground state because it cannot explicitly take into account the very small length-scale effects sampled by an s-like orbital near an impurity ion. Empirical corrections are required, referred to as the central-cell correction. These may take the form of assumed perturbation potentials in the immediate vicinity of the impurity atom [4] that can be compared with both the results of spectroscopic experiments (sensitive to the state energy) and electron nuclear double resonance experiments [5] sensitive to the state's spatial extent [3]. No effective theory has been developed yet to predict both parameters in magnetic fields [3]. Here we focus on the QZE for the ground state, and show that it can be used to extract the spatial extent.

We turn our attention to impurity bound excitons, and their spatial extent. An exciton bound to a neutral impurity is an immobile four-particle complex consisting of two (one) electrons, one (two) hole, and a positive (negative) donor D (acceptor A) ion. A free exciton (X), which consists of an electron and a hole, is analogous to positronium, and, consequently, an impurity bound exciton (donor (D^0X) or acceptor (A^0X)) could be considered an analogue of positronium hydride. The very existence of the D^0X was originally predicted from positronium hydride [6]. The understanding of the magnetic properties of both D^0 and D^0X is crucial for quantum technology applications [7, 8].

The linear Zeeman splitting of the D^0X [9] and A^0X [10] has been studied and good agreement with the theory has been achieved. The QZE has also been observed for D^0X [9] and A^0X [10], but the relatively low magnetic fields used in the reported experimental studies left very high uncertainty in the value of the diamagnetic shifts. In this paper, the luminescence spectra of D^0X are studied up to a magnetic field of 28 T. The luminescence spectral lines result from annihilation of the D^0X into D^0 , so that their magnetic field behaviour depends on the diamagnetic shifts of both D^0X and D^0 . Thus a separate measurement of the D^0 electron ground state diamagnetic shift allows us to extract the exciton diamagnetic shifts from the luminescence spectra. We also extract the g -factors of the electrons, the heavy and the light holes, which are found to be in a very good agreement with EMT and previous low field experimental results. The diamagnetic shifts of heavy and light hole excitons are measured at high precision for the first time here.

2. Theory

Both electrons in the D^0X occupy the singlet wave function (the lowest energy level) and do not contribute to its linear Zeeman energy. The Zeeman energy of the D^0X is therefore entirely determined by the Γ_8 hole, which has $J = 3/2$, i.e. $m = \pm 3/2, \pm 1/2$, for the heavy hole and light hole

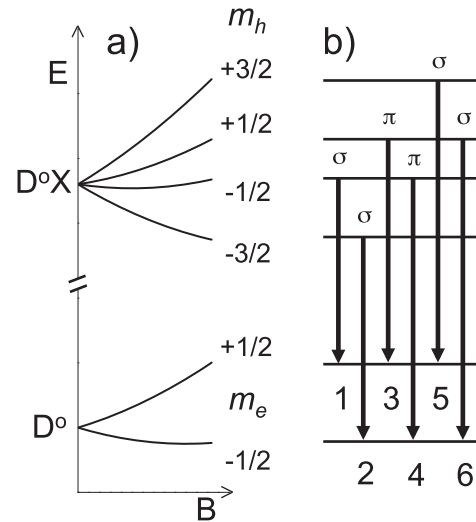


Figure 1. The Zeeman effect in the neutral donor ground state (D^0) and donor bound exciton (D^0X) excited state. (a) The level energies showing both the linear Zeeman splitting at low field and quadratic Zeeman effect (QZE) at high field. The hyperfine coupling with the nucleus has been ignored and the states are labelled with the z -component of the total spin. The top energy levels represent the energy splitting of the D^0X determined by the hole g -factors (initial states); the bottom energy levels are the energy splitting of the ground state of the phosphorus donor (final states). (b) The six possible D^0X optical transitions with polarisation selection rules.

respectively. For high magnetic fields, where the diamagnetic shift becomes significant and results in the QZE, the contribution of all particles (two electrons and one hole) has to be considered.

We begin the discussion of the Zeeman effect with low magnetic fields (for which it is linear), so that the energies of the hole energy levels of the D^0X (figure 1(a)) are

$$E = \pm \frac{3}{2} g_{3/2} \mu_B B \text{ or } E = \pm \frac{1}{2} g_{1/2} \mu_B B. \quad (1)$$

where μ_B is the Bohr magneton, and the transition energy to the D^0 (figure 1(b)) is:

$$\Delta E = E_0 + (m_h g_h - m_e g_e) \mu_B B, \quad (2)$$

where $m_e = \pm 1/2$, $m_h = \pm 3/2$ or $\pm 1/2$ and $g_h = g_{3/2}$ or $g_{1/2}$ depending on the transition (see figure 1).

The values of $g_{3/2}$ and $g_{1/2}$ depend on the direction of the field, and we relate them to the direction-independent band parameters g_1 and g_2 using the spin Hamiltonian of the Γ_8 state, which is the same as the acceptor ground state, and was derived in [11–13] using the shell model [14]:

$$\mathcal{H}_B = \mu_B (g_1 \mathbf{J} \cdot \mathbf{B} + g_2 \sum_i J_i^3 B_i). \quad (3)$$

Here \mathbf{J} is the angular momentum operator, J^3 is the angular momentum projection operator, and i runs over 1, 2, 3. g_1 is the isotropic contribution, and g_2 is the anisotropic correction (symbols K and L were used for g_1 and g_2 in earlier works [15]). For $g_2 = 0$, the paramagnetic contribution to the energies of the states with $m_h = \pm 3/2$ and $m_h = \pm 1/2$ are the same and do not depend on the direction of the magnetic

field. In silicon, due to the angular dependence of the wave function of the hole at the impurity centre, the correction g_2 for the anisotropy differs from zero ($g_2 \neq 0$) and the Zeeman splitting depends on the orientation of the field. The energy levels of the holes in a magnetic field of an arbitrary orientation can be found by diagonalizing the matrix \mathcal{H}_B [13]. The four solutions have the form

$$E = \pm \mu_B B \sqrt{g_M^2 \pm \frac{1}{2} g_D^2 \sqrt{1 - X\beta}}, \quad (4)$$

where the direction of the field determines

$$\beta = \frac{B_x^2 B_y^2 + B_y^2 B_z^2 + B_z^2 B_x^2}{B^4} \quad (5)$$

while the parameters g_M , g_D and X are material specific and related to $g_{1,2}$:

$$g_M^2 = \frac{1}{2} \left[\frac{9}{4} g_+^2 + \frac{1}{4} g_-^2 \right] \text{ and } g_D^2 = \frac{9}{4} g_+^2 - \frac{1}{4} g_-^2, \quad (6)$$

where

$$g_+ = g_1 + \frac{9}{4} g_2 \text{ and } g_- = g_1 + \frac{1}{4} g_2. \quad (7)$$

The anisotropy is determined by X ,

$$X = \frac{9g_2 \left(g_1 + \frac{5}{2} g_2 \right)}{\left(g_1 + \frac{13}{4} g_2 \right)^2} \quad (8)$$

i.e. it is proportional to g_2 , so that for spherical symmetry $X = 0$. Comparing equation (1) with (4), the general g -factors are

$$g_{3/2} = \frac{2}{3} \sqrt{g_M^2 + \frac{1}{2} g_D^2 \sqrt{1 - X\beta}} \\ \text{and } g_{1/2} = 2 \sqrt{g_M^2 - \frac{1}{2} g_D^2 \sqrt{1 - X\beta}}. \quad (9)$$

In the case of \mathbf{B} parallel to [001], i.e. $\beta = 0$, it can be seen from equation (4) that g_M and g_D are the quadrature mean and difference in the slopes of E versus B , and that $g_{3/2} = g_+$ and $g_{1/2} = g_-$, i.e. g_+ and g_- are the heavy and light hole g -values respectively along [001]. For other field directions β is non-zero, e.g. for [111] $\beta = 1/3$ and for [110] $\beta = 1/4$. The quadrature mean of the slopes is unchanged, but the difference is modified.

In the anisotropic case ($g_2 \neq 0$) and for an arbitrary direction of the magnetic field, microwave electron paramagnetic resonance transitions between all levels are allowed. If $\Delta m = \pm 1$ the transition probability is proportional to g_1^2 ; for the other transitions the probability is proportional to g_2^2 . The magnitudes of the parameters g_1 and g_2 were calculated in [16] using a model that considers the interaction of the external magnetic field with hole spin and hole orbital angular momentum including its non-periodic part. A reasonable agreement of the theoretical values with the experimental

results is obtained and shown in table 1. As seen from table 1, the parameters g_1 and g_2 are not only independent of the orientation of the magnetic field, but also independent of the nature of the donor atoms [9, 15]. In order to estimate the g -factors for [110] orientation used in our experiment we have taken average experimental values of g_1 and g_2 , which are also shown in table 1.

In order to describe the magnetic properties of the D^0X luminescence spectra at moderate and high magnetic fields, it is not enough to use only the linear Zeeman splitting. The initial and final energies should also each contain a term quadratic in B , and equation (2) becomes:

$$\Delta E = E_0 + (m_h g_h - m_e g_e) \mu_B B \\ + (b_h^{(D^0X)} - b^{(D^0)}) \cdot B^2, \quad (10)$$

where $b_h^{(D^0X)}$ and $b^{(D^0)}$ are the diamagnetic parameters of the D^0X ($m_h = 3/2; 1/2$) and D^0 . The diamagnetic shift of the multi-electron atom has been derived with first-order perturbation theory for the D^0X [17]:

$$\Delta E = \frac{e^2 B^2}{12} \sum_a \frac{\langle r_a^2 \rangle}{m_a} \quad (11)$$

(in SI units) where e is the electron charge, the sum is taken over all electrons and holes in the D^0X complex, r_a and m_a are the radius vector and the isotropic effective mass of the electron or hole. For 1s-hydrogen-like wave functions we can write $\langle r_a^2 \rangle = 3a_B^2$, where a_B is the Bohr radius. This approximation has been used to estimate the extent of the D^0X wave-functions [10, 18, 19]. We shall show below that this approximation predicts an adequate value only for the diamagnetic shift of D^0 electron but not for D^0X .

3. Experiment

The Si:P sample for D^0X the photo-luminescence experiment was cut from a commercial 800 μm thick silicon wafer from float-zone-grown $\langle 110 \rangle$ monocrystalline natural silicon doped with phosphorus. The level of doping was $2 \times 10^{14} \text{ cm}^{-3}$. The sample was mounted in helium exchange gas at 4.2 K in the bore of a 31.5 T water-cooled Bitter magnet. The direction of the magnetic field was perpendicular to the sample surface (Faraday geometry). The photo-excitation was performed by a Spectra-Physics 2080 argon ion laser ($\lambda = 488 \text{ nm}$), the radiation of which was delivered into the magnet by an optical fibre. Another fibre was used to collect the luminescence from the sample. The spectrum of the luminescence was measured using an Acton Spectrapro 300i monochromator (spectral resolution 0.3 meV) connected to a liquid N_2 -cooled InGaAs array.

A pair of Si:P and Si:Se samples, which are fully described in [20], were used to measure their absorption spectra. The samples were mounted in the same magnet as described above. Mid-infrared radiation from a Fourier transform interferometer (Bruker IFS-113v) was brought to the sample by an evacuated beam line and a focusing cone. An optical window fitted at the bottom of the magnet allowed

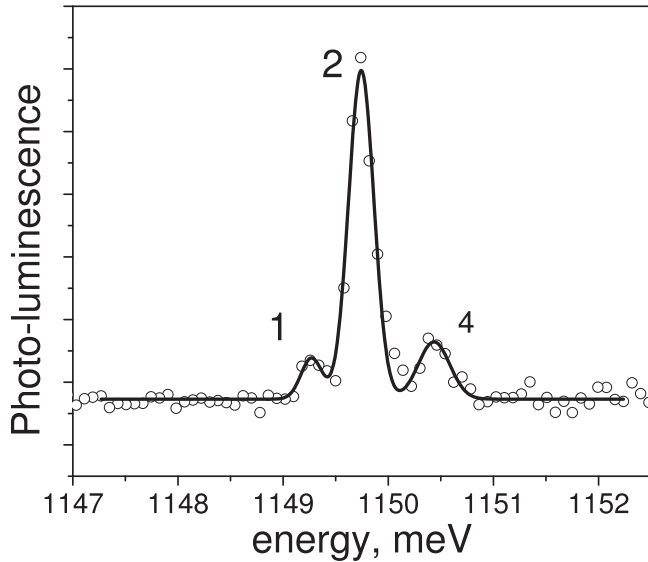


Figure 2. An example of the experimental photo-luminescence spectrum measured at 10 T. The numbers of the resonances indicated correspond to the numbers of the transitions on figure 1. The solid line is a fit with three Gaussians.

us to collect the radiation transmitted through the Si:Se sample by means of an external liquid-nitrogen-cooled MCT detector. The light propagation was parallel to the magnetic field direction and perpendicular to the sample surface (Faraday geometry). For the Si:P sample the transmitted light was detected by a liquid-helium-cooled Si-composite bolometer.

4. Results

Three D^0X lines can be identified in the photo-luminescence spectrum presented in figure 2 at 10 T, one of which is stronger than the others. The amplitude difference can be explained by the occupation probability of the initial states. The recombination time of the D^0X in Si:P is on a few hundred nano-second time scale [21], whereas the intra-complex thermal repopulation is accomplished on a much shorter time scale. Therefore the population of the lowest D^0X energy level with $m_h = -3/2$ is significantly more than that with $m_h = -1/2$. This results in the transition 2 (see figures 1 and 2) being the strongest at high fields. At the sample temperature (4.2 K) the thermal energy $k_B T$ equals the Zeeman splitting at a few tesla (because $g\mu_B/k_B \sim 1 \text{ K T}^{-1}$) which results in complete depopulation of the highest D^0X energy level ($m_h = 1/2$ and $m_h = 3/2$). In the Faraday geometry transition 4, which is π -polarised, should be forbidden (figure 1), but non-sphericity of the ground state and a low f-number of the collection optics have enabled us to detect it. The magnetic field dependence of the transition energies obtained from Gaussian fits to the spectra is shown in figure 3.

First of all, the g -factor of the D^0 electrons can be found by subtracting the field dependence of the transitions 4 and 1

(see figure 3). The result is shown in figure 4. The diamagnetic shifts of the $+1/2$ and $-1/2$ electrons in the D^0 ground states are the same and cancel each other, as do the diamagnetic shifts of the $-1/2$ holes in the D^0X excited states. The result is governed by a linear Zeeman splitting with electron g -factor found to be $g_e = 1.97 \pm 0.01$ (see table 1).

The best global fits to figure 3 with only two fitting parameters ($b_{3/2}$ and $b_{1/2}$, which refer to one of the two possible combinations (equation (10)) of $b^{(D^0X)} - b^{(D^0)}$ values) were achieved for $b_{3/2}(=b_{3/2}^{(D^0X)} - b_e^{(D^0)}) = 2.57 \pm 0.03 \mu\text{eV T}^{-2}$ and $b_{1/2}(=b_{1/2}^{(D^0X)} - b_e^{(D^0)}) = 2.15 \pm 0.03 \mu\text{eV T}^{-2}$ (table 1).

The experimental far infrared absorption spectra of Si:P and Si:Se samples as a function of magnetic field up to 30 T have already been published in [1] and [20], but the analysis to determine the D^0 ground state of Si:P has been done in the present work (figure 5) for the first time.

5. Discussion

It has been shown that the magnetic field behaviour of odd-parity excited states of D^0 is identical for different shallow donor impurity atoms [20]. Subtracting the transition energies from the ground to excited states extracted from the far-infrared absorption spectrum of selenium atoms from the corresponding transition energies of phosphorus atoms allows us to determine the magnetic field behaviour of the phosphorus ground state electron directly. Figure 5 shows the results of such subtraction. The fact that the differences of the corresponding transitions have the same field dependence in all cases confirms that the excited states of Se and P are indeed identical, and that the magnetic field dependence observed in figure 5 results from the ground state shifts only. Due to the very small Bohr radius of the Se ground state electron (0.2 nm for Se in comparison with 1.4 nm for P) its contribution to the diamagnetic shift shown in figure 5 is negligibly small (see equation (11)). Therefore the observed shift is purely determined by field tuning of the phosphorus ground state. From the fitting of the experimental data shown in figure 5 the diamagnetic coefficient of phosphorus ground state electron is found to be $b_e^{(D^0)} = 0.26 \pm 0.02 \mu\text{eV T}^{-2}$, which implies that (equation (11)) we found that $a_B = 1.33 \pm 0.05 \text{ nm}$. Our experimental diamagnetic coefficient is in good agreement with the previously reported value of $0.3 \mu\text{eV T}^{-2}$ obtained using first-order perturbation theory from (equation (11)) and assuming $a_B = 1.5 \text{ nm}$ [19], although different theoretical models for the state radius predict a_B from 0.65 to 2.5 nm (for review see [3]), which leads obviously to considerable theoretical uncertainty in b . A numerical calculation of the diamagnetic shifts of the ground and excited states of shallow donors in silicon, that included only one conduction-band valley, found the ground state shift to be $0.353 \mu\text{eV T}^{-2}$ [22]. If a linear combination of six single-valley states is considered, the diamagnetic shift is reduced. Because of this reduction it was assumed in [22] that the diamagnetic shift of the ground state could be neglected in comparison with that of the excited states. Our experimental

Table 1. g factors and diamagnetic parameter for electrons (g_e , b_e) and holes.

Field dir ⁿ	Source	Dopant	Max field, T	g_e	$g_{1/2}$	$g_{3/2}$	g_1	g_2	$b_{1/2}$ $\mu\text{eV T}^{-2}$	$b_{3/2}$ $\mu\text{eV T}^{-2}$	b_e $\mu\text{eV T}^{-2}$
Theory											
	[19]										0.3
	[22]										<0.353
$\langle 001 \rangle$	[16]				0.97	1.22	0.93	0.13			
Experiment:											
$\langle 001 \rangle$	[9]	P	5	2.04	0.86	1.33	0.80	0.24	1.6	2.1	
	[15]	As	9	1.85	0.79	1.24	0.74	0.22	1.85	1.85	
	[24]	P	0.05	1.97	0.83	1.3					
$\langle 111 \rangle$	[9]	P	5	1.99	1.54	1.27	0.86	0.21	1.5	3.4	
	[15]	As	9	1.85	1.46	1.17	0.74	0.22	1.85	1.85	
$\langle 110 \rangle$	[15]	As	9	1.85	1.31	1.19					
Average values											
		P		2.00			0.83 ^a	0.225 ^a			
		As		1.85			0.74	0.22			
This work											
$\langle 110 \rangle$		P	28	1.97	1.409 ^a	1.285 ^a	0.83 ^a	0.225 ^a	2.15	2.57	0.26

^a Average $g_{1,2}$ values were taken from [9], and $g_{1/2, 3/2}$ were calculated from them using equations (4)–(8), rather than using them as fit parameters.

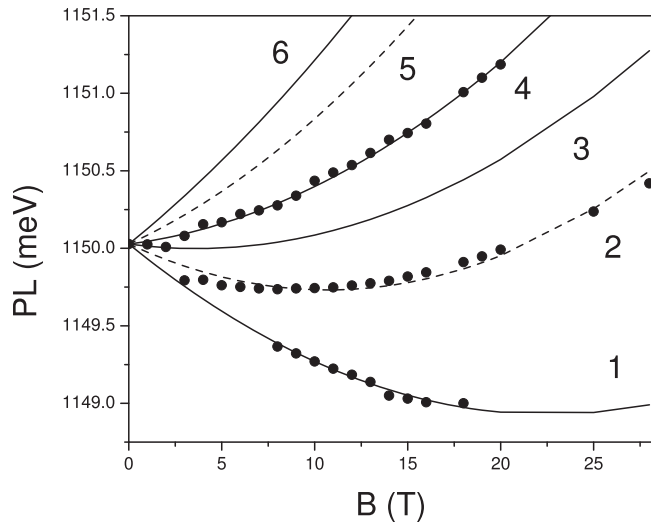


Figure 3. The magnetic field dependence of the transition energies from spectra at fixed fields such as figure 2. The lines are fits where $g_{3/2}$ and $g_{1/2}$ are taken from previous work and there is one free parameter ($b_{3/2} = b_{3/2}^{(D^0X)} - b_e^{D^0}$) for the dashed lines which are heavy hole transitions, and one ($b_{1/2} = b_{1/2}^{(D^0X)} - b_e^{D^0}$) for the solid lines, light holes.

results show that although it is small it is non-negligible; it is 9% (7%) of that of $2p_0$ ($2p_{\pm}$) states. Ignoring it, in order to analyse experimental magnetic field behaviour of the excited states, results in under-estimation of the magnetic field effect on the latter. The discrepancy with the experiment becomes unavoidable at high magnetic field [1] if the diamagnetic shift of the electron ground state is neglected.

Only a few experimental studies of the diamagnetic shift of the D^0X are available in the literature; most are summarised in table 1. In [15] the authors quoted the precision of the observed diamagnetic shift to be 4%, but they took all

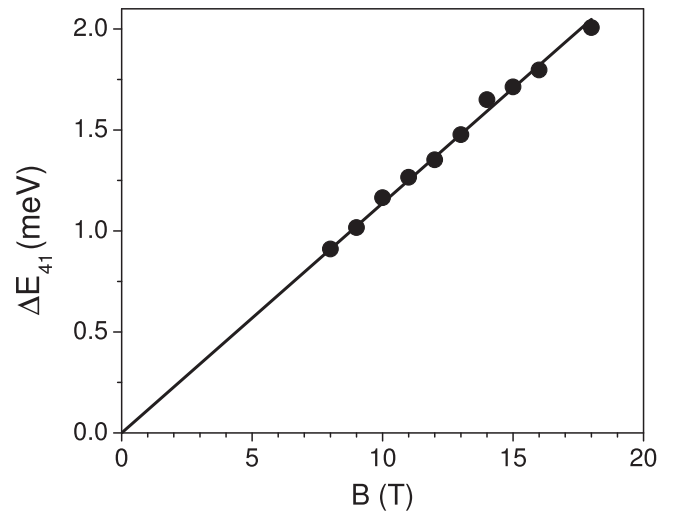


Figure 4. The difference in transition energies for lines 4 and 1 (see figures 2 and 3), which is equal to the electron spin splitting.

heavy and light hole D^0X diamagnetic shifts to be the same. Data of the same field range as in [15] was treated separately in [9] and a more realistic precision of the order of 25% was reported. Our high magnetic field experiments allow us to measure the diamagnetic shifts with high precision (~1%).

Using the diamagnetic coefficients extracted from figure 3 ($b_{3/2}$ and $b_{1/2}$) and the D^0 diamagnetic coefficient ($b_e^{(D^0)}$) extracted from figure 5, we can now estimate the heavy and light hole D^0X diamagnetic coefficient, which are found to be $b_{3/2}^{(D^0X)} = 2.83 \pm 0.04$ and $b_{1/2}^{(D^0X)} = 2.41 \pm 0.04$ for the heavy and light hole D^0X respectively. The calculation of the Bohr radii of two electrons and one either heavy or light hole in the D^0X was performed in [23] using the variational method. Substituting their results in equation (11) and using the effective masses of free electrons and holes, gives $b_{3/2}^{*(D^0X)} = 0.77$ and $b_{1/2}^{*(D^0X)} = 1.8$. These theoretical values

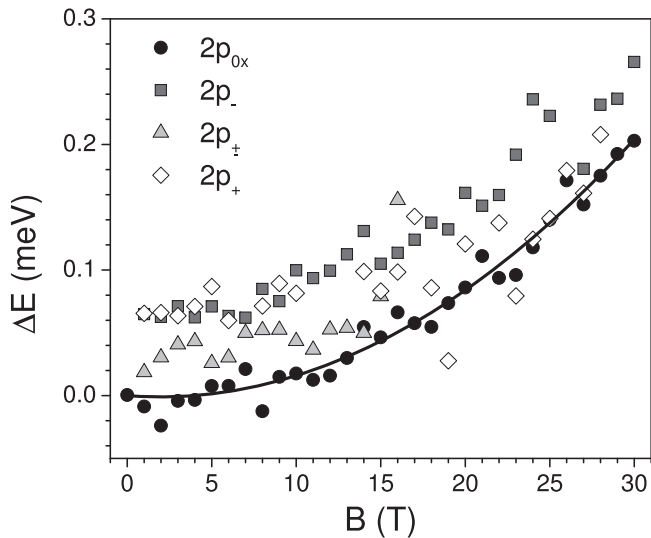


Figure 5. The orbital contribution to the energy of the ground state of the Si:P D^0 (data from [20]). The THz absorption transition energy for $1s(A_1) - >2p_0$ of Si:Se was subtracted from the energy of the equivalent transition in Si:P (and the same for three other transitions involving different excited states). The excited states in both Si:P and Si:Se are identical [20], and the Si:Se ground state has negligible QZE due to its small extent, therefore the field dependence revealed in the figure is entirely due to the QZE in the ground state of the Si:P D^0 state.

have the same order of magnitude, but opposite relative strength ($b_{1/2}^{*(D^0X)}/b_{3/2}^{*(D^0X)} = 2.3$), which contradicts our experimental result ($b_{1/2}^{(D^0X)}/b_{3/2}^{(D^0X)} = 0.85 \langle 011 \rangle$) and earlier low field estimates in the literature ($b_{1/2}/b_{3/2} = 0.76 \langle 001 \rangle$ and $b_{1/2}/b_{3/2} = 0.44 \langle 111 \rangle$) [9]. It is well known that a particle with a larger effective mass is expected to have a smaller Bohr radius. If we apply this simple logic to equation (11) we might expect the heavy hole D^0X diamagnetic coefficient to be smaller than that of the light hole D^0X , which is exactly the opposite to our experimental observation. This illustrates the need to include heavy-light hole mixing to explain the relative orbit sizes.

6. Conclusion

The diamagnetic shift of the hydrogen-like neutral donor ground state electron has been obtained experimentally for the first time. We showed that the magnitude of the diamagnetic shift is well described within the EMT and that $b_e^{(D^0)}$ is about 9% (7%) of that of $2p_0$ ($2p_{\pm}$) states, which shows that the magnetic field dependence of the electron ground state cannot be neglected especially for impurity magneto-optics at high magnetic field.

We studied the magneto-optics of the more complicated particle, the donor bound exciton, up to high magnetic field (28 T). At low fields the Zeeman splitting is linear and gives good agreement with the EMT—the measured electron and hole g -factors agree with previous results. At high magnetic fields where the QZE becomes important, the diamagnetic shift of the light and heavy holes are found to contradict the EMT, which predicts that it should be proportional to the

square of the state radius. The $m_J = \pm 3/2$ D^0X radius is found to be larger than that of the $m_J = \pm 1/2$ light holes. A similar experimental trend in diamagnetic shifts has been reported in the literature [9], but not discussed due to low precision of the existing low field experimental data. The field for which the energy associated with the QZE is equal to that of the linear Zeeman effect for holes in silicon ($g_h \mu_B / b$) is found to be of ~ 30 T, and this sets the field scale required for accurate extraction of b . The high magnetic field used in our work allowed us to improve the precision by over an order of magnitude. Clearly, a more accurate theory for such objects at high magnetic field has to be developed, that includes heavy-light hole mixing [25].

Acknowledgments

This work was supported by the EPSRC-UK [COMPASSS, Grant No. EP/H026622], and the research programme of the ‘Stichting voor Fundamenteel Onderzoek der Materie (FOM)’, which is financially supported by the ‘Nederlandse Organisatie voor Wetenschappelijk Onderzoek (NWO)’. BNM is grateful for a Royal Society Wolfson Research Merit Award.

The raw data used in this work are available to download at 10.5281/zenodo.44977.

References

- [1] Murdin B N *et al* 2013 *Nat. Commun.* **4** 1469
- [2] Luttinger J M and Kohn M 1955 *Phys. Rev.* **97** 869
- [3] Hui H T 2013 *Solid State Commun.* **154** 19
- [4] Ning T H and Sah C T 1971 *Phys. Rev. B* **4** 3468
- [5] Hale E B and Mieher R L 1969 *Phys. Rev.* **184** 751
- [6] Lampert M A 1958 *Phys. Rev. Lett.* **1** 450
- [7] Steger M, Saeedi K, Thewalt M L W, Morton J J L, Riemann H, Ambrosimov N V, Becker P and Pohl H-J 2012 *Science* **336** 1280
- [8] Saeedi K, Simmons S, Salvail J Z, Dluhy P, Riemann H, Ambrosimov N V, Becher P, Pohl H-J, Morton J L and Thewalt M L W 2013 *Science* **342** 830
- [9] Kaminskii A S, Karasyuk V A and Pokrovskii Y E *Sov. Phys. —JETP* **52** 211
- [10] Karasyuk V A, Brake D M and Thewalt M L W 1993 *Phys. Rev. B* **47** 9354
- [11] Bleaney B 1959 *Proc. Phys. Soc.* **73** 939
- [12] Luttinger J M 1956 *Phys. Rev.* **102** 1030
- [13] Bir G L and Pikus G E 1972 *Symmetria and deformationnyye efekty v poluprovodnikakh (Symmetry and Deformation Effects in Semiconductors) (Nauka, M.)* p 538
- [14] Kirczenow G 1977 *Solid State Commun.* **21** 713
Kirczenow G 1977 *Can. J. Phys.* **55** 1787
- [15] Cherlow J M, Aggarwal R L and Lax B 1973 *Phys. Rev. B* **7** 4547
- [16] Suzuki K, Okazaki M and Hasegawa H 1964 *J. Phys. Soc. Japan* **19** 930
- [17] Landau L D and Lifshitz E M 1974 *Quantum Mechanics* (Oxford: Pergamon)
- [18] Kulakovskii V D, Malyavkin A V and Timofeev V B 1979 *Zh. Eksp. Teor. Fiz.* **77** 752
Kulakovskii V D, Malyavkin A V and Timofeev V B 1979 *Sov. Phys.—JETP* **50** 380

- [19] Kulakovskii V D, Malyavkin A V and Timofeev V B 1979 *Zh. Eksp. Teor. Fiz.* **76** 272
Kulakovskii V D, Malyavkin A V and Timofeev V B 1979 *Sov. Phys.—JETP* **49** 139
- [20] Litvinenko K L *et al* *Phys. Rev. B* **90** 115204
- [21] Schmid W 1977 *Phys. Status Solidi b* **84** 529
- [22] Thilderkvist A, Kleverman M, Grossmann G and Grimmeiss H G 1994 *Phys. Rev. B* **49** 14270
- [23] Suffczynski M and Wolniewicz L 1989 *Phys. Rev. B* **40** 6250
- [24] Yang A *et al* 2006 *Phys. Rev. Lett.* **97** 227401
- [25] Ivchenko E L and Kaminski A Y 1996 *Phys. Rev. B* **54** 5852